Tunable High-Q TSV Inductor Packaging with MEMS

Bruce Kim*, Saikat Mondal*, Sang-Bock Cho**

*Department of Electrical Engineering, City University of New York,
New York, USA
Bruce.Kim@ieee.org
**EE department, Ulsan University
Ulsan, South Korea

Downloaded from http://meridian.allenpress.com/ism/article-pdf/2015/1/000062/2256558/isom-2015-tp26.pdf by guest on 29 November 2022

Abstract

In this paper, we present a Through-Silicon-Via (TSV)-based 3D tunable inductor implementation for RF applications. The proposed inductor structure uses MEMS (Micro Electro-Mechanical Systems) switches to vary inductance by activating and deactivating the switches. MEMS-based switches are used to offer high isolation in the off state. The tunable inductor is tested within an LNA circuit for variation in off-state leakage resistance. Detailed 3D full wave simulation results are presented for different cellular frequency bands.

Key words

TSV, inductor, MEMS, tunable inductor, 3D inductor

I. Introduction

3D chip stacking has emerged as a potential key to realizing small RF components that require disparate technologies within reduced package size. The use of metal-filled Through Silicon Via (TSV) as an interconnect among different dies has increased package density dramatically. Now inductors, an integral RF component, can also be realized using TSVs. This will result in reducing the footprint of the inductor on the die and making the inductance density per unit area much higher than that of the conventional 2D on-chip spiral inductors [1].

TSV-based inductors have parasitic components that limit the self-resonance frequency and quality factor of the inductor. The quality factor of an inductor can be derived as in (1). Here EM is the peak magnetic energy, EC is the peak capacitive energy and ER is the energy loss in one cycle. The quality factor of an inductor denotes how efficiently total energy can be stored as magnetic energy. Hence, for a better quality factor, the capacitance and resistance of the inductor should be as small as possible. Various methods have been adopted to enhance the quality factor, namely [2] and [4] for 2D inductors and [1] and [3] for 3D inductors. To enhance the quality factor, various methods such as the use of a highly resistive substrate, materials with low loss tangent and low dielectric constant in place of SiO2, and even different conductors such as CNT in place of Cu have been explored. As the frequency of operation increases, a frequency is reached where electrical energy equals magnetic energy. This particular frequency is called the self-resonance frequency of the inductor, at which the quality factor becomes zero. Further above this self-resonance frequency, the inductor behaves as a capacitor, as the stored electrical energy is greater than the magnetic energy.

$$Q = 2\pi \times \frac{E_M - E_C}{E_R} \qquad (1)$$

On-chip inductors can be used in applications such as various filters and LNAs. Tunable inductors are useful in selecting specific bands for implementation and controlling the gain in LNAs according to the requirements. In wireless systems, multiple frequency bands are used for voice and high-speed data communication. Hence tunability is very important to implement a multiple band selective filter. Investigating the prospects of tunable inductor design in the context of a 3D TSV inductor is therefore of interest.

Switches are essential to implementing the required inductor adjustment. In this paper, MEMS-based switches are proposed in place of conventional MOSFET-based switches to offer high isolation at the off state. The tunable inductor is tested in a Low Noise Amplifier (LNA) with MOSFET and MEMS switches to compare performance.

The paper is structured as follows: we first present a 3D

inductor realized using an EM simulator; with the simulation result, a variable inductor is then realized using a circuit simulator in section II. A detailed MEMS-based cantilever structure for the switch implementation is described in section III. The paper is concluded in section IV.

II. Approach

A. Tunable Inductor Design

Several papers have reported on tunable 2D on-chip inductors using various configurations of MOSFET switching. The conventional designs [5, 6] used for switch inductors are illustrated in Figures 1 and 2. Pham [6] demonstrated that the model used by Park [5] is inefficient in properly sorting the inductor at the on state of the MOSFET switch. However, in Pham's model, 2n numbers of control units are augmented for additional n numbers of inductor segments. Off-state non-zero leakage current is one of the major problems with MOSFET-based switches. Due to the leakage current from drain to source, there is always unwanted power loss, which can be recovered using MEMS-based switches.

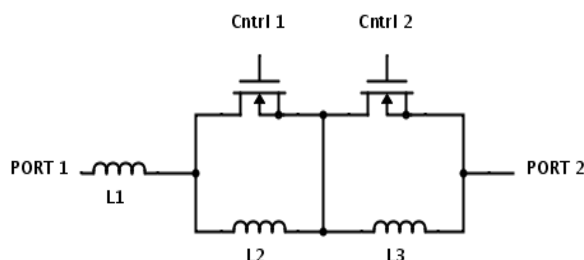

Figure 1. Conventional model 1 for variable inductance [5].

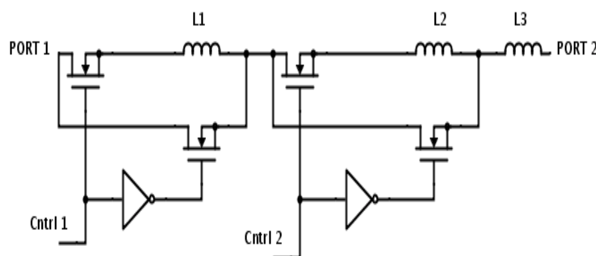

Figure 2. Conventional model 2 for variable inductance [6]
.

The model presented in this paper optimizes the number of switches within the inductor segments and optimizes the area required to implement MEMS cantilevers. The model also completely cuts off the target inductor from the residual circuit at the off state. Assuming L1=L2=L3=L4=L, the equivalent inductance between port 1 and port 2 in Figure 3 is summarized in Table 1 using the control switches.

Table 1. Equivalent Inductance for Different Control Inputs

Control 1	Control 2	Equivalent Inductance
Low	Low	2L
High	Low	3L/2
Low	High	3L/2
High	High	L

The 3D inductor structure illustrated in Figures 4 and 5 is compatible for TSV fabrication. Its particular orientation helps to minimize the required TSV area. The unit TSV inductor structure with N=2 number of turns was simulated in the EM simulator, and the S-parameter values from which passive components can be extracted were exported in touchstone format to be read by the circuit simulator to obtain the inductance and quality factor for behavioral modeling.

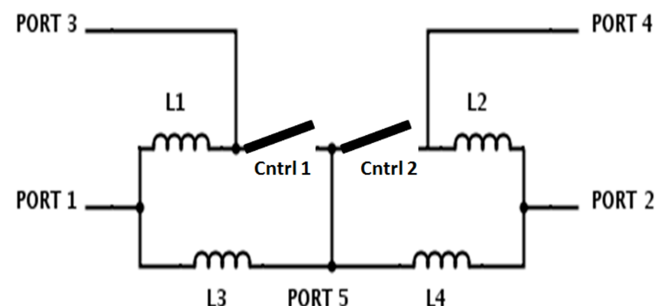

Figure 3. Proposed model for variable inductance.

B. TSV-Based Spiral Inductor

To model a TSV-based inductor, the key control factors are the diameter and length of the TSV, the distance (D) between two unit inductors and the length (L), width (W) and thickness of the metal interconnects. In most cases, the diameter and length of the TSV and the thickness of the metal interconnects are limited by the foundry process. However, a thickness up to 8 μm for the metal layer can be considered in specific cases [6]. Due to mechanical stress, spacing D has a certain minimum threshold limit [7]. The substrate is assumed to be bulk silicon, which is conductive. Hence a separation layer of SiO_2 is maintained between the metal and the silicon layers. The parameters considered in the design are summarized in Table 2.

Downloaded from http://meridian.allenpress.com/ism/article-pdf/2015/1/000062/2256558/isom-2015-tp26.pdf by guest on 29 November 2022

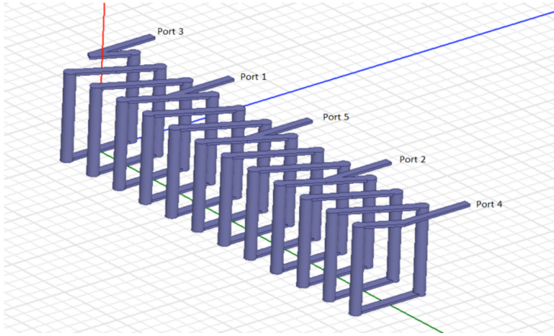

Figure 4. 3D TSV inductor model with N=12.

Table 2 Design Parameters for TSV and Metal Interconnect

Design Parameters	**Control 2**
TSV length	300 µm
TSV diameter	40 µm
Metal Width	25 µm
Metal Thickness	8 µm
Minimum Spacing D	125 µm

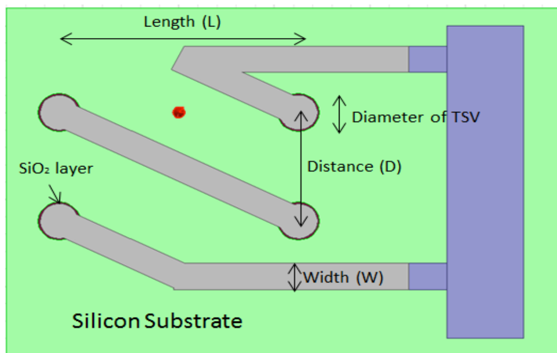

Figure 5. Top view of a 3D TSV inductor with N=2 number of turns.

C. MEMS-Based Switch Design

As mentioned earlier, the switch was designed using MEMS. A magnetically actuated switch was chosen for its high speed and insulation capability in the presence of high voltages. The design consists of a cantilever bridge structure, a permanent magnet and an electrostatically actuated coil magnet. The working principle of the switch can be described in terms of the magnetic force acting on it when dc voltage is applied [8]. When the voltage is low, the MEMS switch is closed, completing the circuit under the permanent magnet force. When the dc voltage is high, the coil magnet negates the force produced by the permanent magnet. Hence the switch is in the open position. The total force exerted on each switch is largely dependent upon the intensity of the magnetic field produced by the external permanent magnet and the electromagnetic coil, the volume of the ferromagnetic material embedded on the bridge and the spring constant of the flexible bridge. The force exerted by the magnet on the beam during the closed state is given in (2).

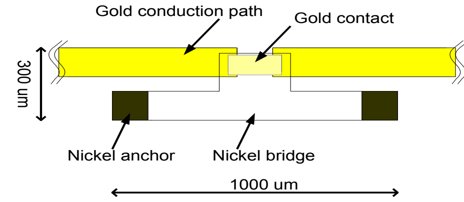

Figure 6. Plan view of the MEMS switch [8].

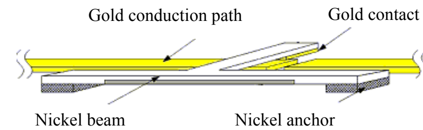

Figure 7. Isometric view of the MEMS switch in the open switch position [8].

Figure 8. Isometric view of the MEMS switch in the closed switch position [8].

$$F_Z = \frac{dw_m}{db} \qquad (2)$$

where w_m is the total energy in the magnetic fields, and b is the gap between the two. The variable magnetic energy is dominated by the energy

$$w_m = \mu_0 H_{gap}^{\ 2} \frac{bA}{2} \qquad (3)$$

where A is the area of the permanent magnet's surface. Therefore the force is given by

$$F_Z = \mu_0 H_{gap}^{\ 2} \frac{A}{2} \qquad (4)$$

The nickel beam is 1000 µm long, 100 µm wide and 4 µm thick.Hence the uniform pressure required to bend a doubly clamped beam is given by [1].

$$P = \left(\frac{\pi^4}{3}\right)\left[\frac{EH^3}{L^4}\right]c + \left(\frac{\pi^4}{4}\right)\left[\frac{EH}{L^4}\right]c^3 \quad (5)$$

where

E = Young's modulus of nickel = 214 GPa

H = height of the beam (thickness) = 4 µm

L = length of the beam = 1000 µm

c = deflection of the beam = 1.5 µm

Downloaded from http://meridian.allenpress.com/ism/article-pdf/2015/1/000062/2256558/isom-2015-tp26.pdf by guest on 29 November 2022

Therefore the force required to obtain a deflection of 1.5 µm is 75 µN. However, applied force of at least 500 µN is required to reduce the contact resistance. Figure 5 shows the finite element analysis of the switch to estimate the stress experienced by the beam, obtained with the Xansys CAD tool. The beam was subjected to force for stress analysis. The shade scale exhibits the amount of stress experienced by various parts of the beam. The analysis concluded that the beam can reliably withstand force in the range of 800 to 1200 µN. Hence the external magnetic field required to generate the force is around 0.07 T.

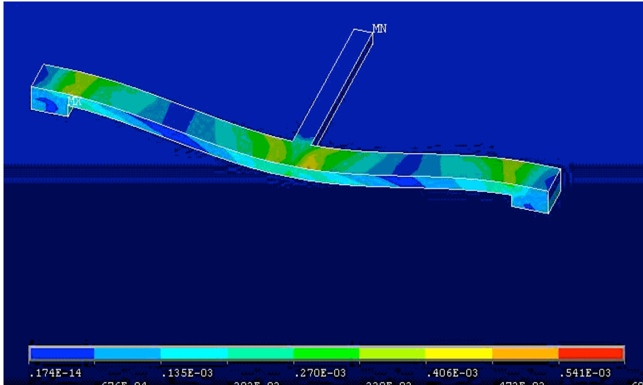

Figure 9. Mechanical Simulation of the MEMS Bridge [8].

III. Results

Various simulations were performed in the EM simulator on a unit TSV inductor structure by varying the length (L) and width (W) of the metal interconnect. From the simulation results, it is evident that increasing the metal interconnect length results in a decrease in the self-resonant frequency and a simultaneous decrease in the quality factor. When the width of the metal interconnect is increased, the quality factor improves. However, this results in a lower inductance value.

At a higher frequency, the resistance from the skin effect becomes dominant, which decreases the quality factor. Again, the longer the metal track length, the higher the inductance value, but resistance also increases.

The inductance and quality factor of the inductor are calculated from the Y parameters as follows using (1) and (2).

$$L = \frac{\mathrm{Imag}[1/Y_{11}]}{2\pi f} \qquad (6)$$

$$Q = \frac{\mathrm{Imag}[1/Y_{11}]}{\mathrm{Real}[1/Y_{11}]} \qquad (7)$$

The length and width of the metal tracks are to be varied to find the optimum inductance and quality factor.

The closed position using the MEMS switch array is presented in Figure 10. The turn-on time response is one of the important parameters for determining the characteristics of the MEMS switch. The delay of the switch is calculated as the difference in t_{50} of the trigger voltage and the output voltage. The Turn ON and Turn OFF times measured for the MEMS switch were 426 µs and 328 µs, respectively.

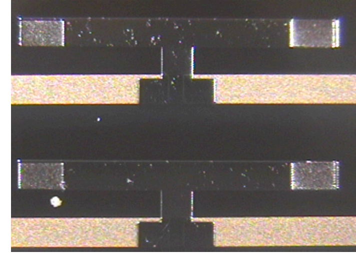

Figure 10. A 4X4 MEMS switch array in the closed position [8].

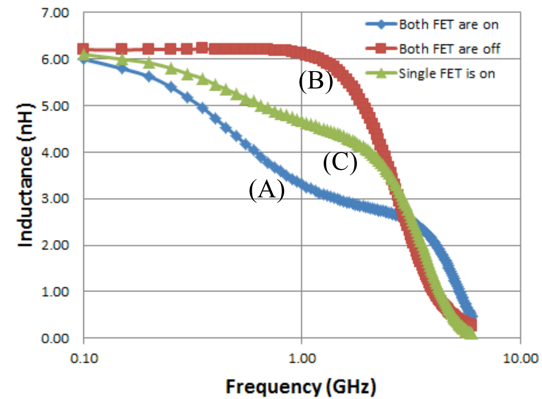

Figure 11. Inductance with N=12 for different switching operations: (A) Both FETs are on; (B) Both FETs are off; (C) A single FET is on.

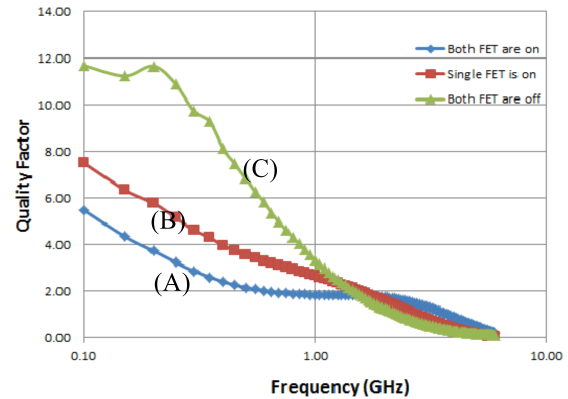

Figure 12. Quality factor for different switching operations (A) Both FETs are on; (B) A single FET is on; (C) Both FETs are off.

The most widely used GSM bands are from 700 MHz to 2.1 GHz. However, the LTE (Long Term Evolution) spectrum lies from 700 MHz to 3.8 GHz. Hence our study of inductance and quality factor response has been limited to the range from 100 MHz to 6 GHz.

Downloaded from http://meridian.allenpress.com/ism/article-pdf/2015/1/000062/2256558/isom-2015-tp26.pdf by guest on 29 November 2022

TABLE 2 SUMMARY OF RESULTS AT THE 700 MHZ LTE BAND

Control 1	Control 2	Inductance	Quality Factor
Low	Low	6.19 nH	4.98
High	Low	4.94 nH	3.11
Low	High	4.94 nH	3.11
High	High	3.78 nH	1.94

TABLE 3 SUMMARY OF RESULTS AT THE 900 MHZ GSM BAND

Control 1	Control 2	Inductance	Quality Factor
Low	Low	6.15 nH	3.78
High	Low	4.74 nH	2.81
Low	High	4.74 nH	2.81
High	High	3.43 nH	1.87

In Tables 2, 3 and 4, the inductance and quality factor values are summarized for popular frequency bands. From the concise values, it is apparent that TSVs would be very useful for realizing tunable filters within cellular frequency bands.

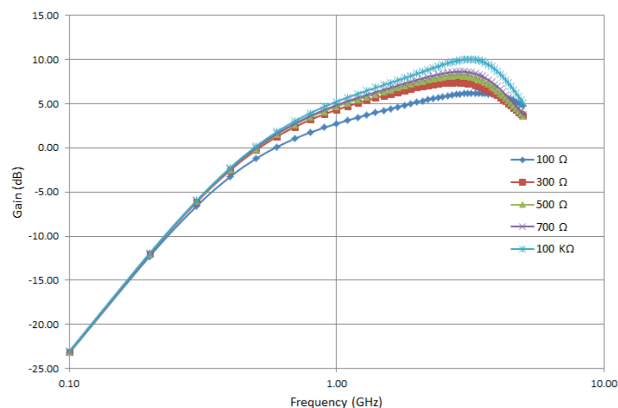

Figure 13. Gain for different levels of off-state leakage resistance for the MOSFET switch.

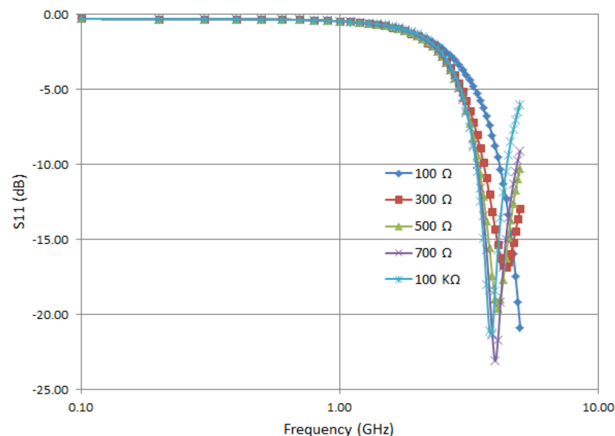

Figure 14. Reflection coefficient for different levels of off-state leakage resistance for the MOSFET switch.

The tunable inductor was tested for a Low Noise Amplifier (LNA) circuit to compare the performance of the MEMS and MOSFET switches. The LNA is designed for application at 3 to 4 GHz. Figures 13 and 14 show that the MEMS switch performance is better than the high leakage off-state MOSFET switch in terms of gain and reflection coefficient. For the low value off-state resistance of the MOSFET switch, the gain in LNA is found to be degraded.

IV. Conclusions

In this paper we proposed a tunable inductor based on 3D TSV structure and MEMS switches. The inductance varies from 6 nH to 3 nH at 1 GHz depending upon the switching operation. MEMS-based switches are proposed in this design to offer high isolation, which the MOSFET switches lack due to the leakage current in the switch's off state.

Acknowledgments

This work is partially supported by the Semiconductor Research Corporation (SRC) through the Texas Analog Center of Excellence at the University of Texas at Dallas (Task ID: 1836.123). We are grateful to NOAA-CREST Center for their assistance with software tools.

References

[1] U. Tida et al., "Through-silicon-via inductor: Is it real or just a fantasy?" Design Automation Conference (ASP-DAC), 19th Asia and South Pacific, pp. 20-23 Jan. 2014.

[2] M. Rais-Zadeh , J. Laskar and F. Ayazi, "High performance inductors on CMOS-gradetrenched silicon substrate", IEEE Transaction on Components, Packaging and Manufacturing Technology, vol. 31, no. 1, pp.126-134, 2008.

[3] W. A. Vitale , M. Fernandez-Bolanos and A. M. Ionescu, "High-Q 3D embedded inductors using TSVfor RF MEMS tunable bandpass filters (4.65-6.8 GHz)", Proceedings of European Microwave Integrated Circuits Conference, pp.822-825, 2012.

[4] S. Jenei et al., "High Q inductor add-on module in thick Cu/SILK™ single damascene", Proceedings of IEEE International Interconnect Technology Conference, pp. 107–109, 2001.

[3] P. Piljae, C. Kim, P. Y. Mun, S. D. Kim and H. K. Yu, "Variable inductance multilayer inductor with MOSFET switch control," Electron Device Letters, IEEE , vol.25, no.3, pp.144,146, 2004.

[4] D. P. Khoa, K. Okada and K. Masu, "On-chip variable inductor using MOSFET switches," European Microwave Conference, vol.2, pp. 4-6, 2005.

[5] C. Bousey, "Design and realizations of integrated filters on silicon for TV on mobile," in Proc. Of National Micro-Wave Days, (JNM 07), pp.1-4, 2007.

[8] R. Kasim, B. C. Kim, and J. Drobnik, "Advanced MEMS for high power integrated distribution systems," International Conference on MEMS, NANO and Smart Systems, pp. 247-254, 2005.

Downloaded from http://meridian.allenpress.com/ism/article-pdf/2015/1/000062/2256558/isom-2015-tp26.pdf by guest on 29 November 2022